Available online at www.sciencedirect.com

ScienceDirect

Procedia Manufacturing 10 (2017) 662 – 673

Procedia MANUFACTURING

45th SME North American Manufacturing Research Conference, NAMRC 45, LA, USA

Quality enhancement with ultrasonic wave and pulsed current in electrochemical machining

Jigar B. Patel[a], Zhujian Feng[a], Pedro P. Villanueva[b], and Wayne N.P. Hung[a]* †

[a] *Texas A&M University, College Station, Texas, USA*
[b] *COMIMSA, Saltillo, Mexico*

Abstract

This paper presents the results of enhancement in Electrochemical Machining (ECM) by combining pulsed current and ultrasonic wave in flowing electrolyte through an electrode. Teflon coated stainless steel tubes were used as electrodes to produce deep holes in 6061-T6 aluminum. Material removal rate and hole quality were measured on a 3D optical profiler to study the effect of pulsed current amplitudes, pulsed frequencies, machining times, and ultrasonic wave amplitudes. Although pulsed current improves the removal rate, cavitation induced microjet suppresses the ionization process. The shockwaves from busting of cavitated bubbles break the aluminium tribromide by-product into fine powder that flows and polishes the workpiece surface. Although ultrasonic wave at 40 kHz compromised material removal rate, it significantly enhances the part quality by reducing surface roughness from 2.5 µm to 1 µm. The combined effect of pulsed current and ultrasonic wave reduces taper angle of ECM'ed holes sidewall from ~11° to 1°.

Peer-review under responsibility of the organizing committee of the 45th SME North American Manufacturing Research Conference

Keywords: Ultrasonic enhancement, Electrochemical machining, Surface roughness, Pulsed current

1. Introduction

Electrochemical machining (ECM) is a machining technique based on the principle of anodic dissolution. When two electrically conductive materials are placed in close proximity in the presence of an electrolytic fluid that conducts ions, the anodic workpiece releases ions towards the cathodic electrode. If the newly formed ions in

* Corresponding author. Tel.: +1-979-845-4989; fax: +1-979-862-7969.
E-mail address: hung@tamu.edu

Peer-review under responsibility of the organizing committee of the 45th SME North American Manufacturing Research Conference
doi:10.1016/j.promfg.2017.07.013

electrolyte are not effectively flushed away from an anode surface, the cumulative ions would be stagnant and inhibit further ion dissolution, therefore, affecting material removal rate and the quality of an ECM'ed component. Effective removal of by-products is a challenge when high aspect ratio features are fabricated by ECM. Researchers have attempted to vibrate either electrode or workpiece at different frequencies to enhance the process but with limited success, therefore, an alternative approach is sought to further improve material removal rate and surface finish. The objectives of this research are to (i) integrate ultrasonic wave into flowing electrolyte to improve ion flushing, and (ii) study the combined effect of ultrasonic and pulsed current on ECM material removal rate and part quality.

2. Literature review

The Faraday's law of electrolysis was proposed in 19th century to predict the mass removal in an electrolytic system:

$$m = \frac{Q}{F}\frac{M}{z} = \frac{It}{F}\frac{M}{z} \tag{1}$$

Where

m	: removed mass (g)
Q	: electrical charge (Coulomb)
F	: Faraday's constant = 96500 Coulomb/mole
M	: molecular mass of anode (g/mole)
z	: valence electron of anode
I	: current (A)
t	: time (s)

The original Faraday's work used direct current for electrolytic plating; it assumed the removal rate of anodic ion is the same with the rate for ion depositing on cathode, and chemical replenishing rate. Although an electrolyte can be static in theory, it is commonly pumped at high flowing rate to flush away the debris, reduce the electrolyte temperature, and replenish fresh chemical species between electrodes. Researchers have been investigating techniques to enhance ion transport in electrolysis to improve material removal rate (MRR) and quality of parts produced by ECM. Pulsed current provides necessary and addition time for debris flushing; ultrasonic wave can break agglomerated by-products by cavitation action therefore enhance flushing action. Different techniques have seen in published literature.

- Use of pulsed current in ECM.

Continuous direct current (DC) heats the electrolyte between electrodes due to high resistance of inter-electrode gap. This unavoidable thermal energy would affect the machining accuracy and product quality.

The use of pulsed current was proposed to improve dimensional accuracy by reducing the electrolyte temperature, allowing time for flushing of machining by-products away from inter-electrode gap [1]. In reference [2], it was proposed that the parameters of pulsed current (pulsed on-time, pulse off-time and peak current density) may be manipulated in order to obtain trade-off desired MRR and heat generated during operation.

- Vibration of workpiece or electrode.

Low frequency vibration of workpiece or electrode is an attempt to cyclically alter the electrode gap and enhance flushing. Because ultrasonic wave is an effective method to break agglomerated by-products in chemistry, the use of ultrasonic wave has been proposed to enhance the flushing of by-products in ECM. Previous research in incorporating ultrasonic enhancement to ECM has been either through vibration of tool or workpiece.

The ultrasonic vibration of the tool narrows the inter-electrode gap and then widens it periodically. This causes the machining by-products to be forced out and fresh electrolyte to pour into the gap periodically for effective flushing. The authors in reference [3] studied the influence of ultrasonic vibration of electrode; they concluded that ultrasonic vibration frequencies between 3-23 kHz was not significantly affect MRR and overcut of ECM'ed microholes. High ultrasonic frequency however would produce encouraging results. In references [4-6] the authors studied the influence of ultrasonic and magnetic fields on ECM in an attempt to achieve superfinishing. Tool vibration at very high frequencies (46-120 kHz) and power (50-80 W) was applied to ECM. It was found that the highest frequency of 120 kHz and power of 80 W produced an average surface finish of 0.4 µm. In another study, the author used a rotating workpiece and different designs of electrode along with ultrasonic vibration and pulsed DC current. The frequency and power of ultrasonic vibrations were ranging from 46-120 kHz and 50-150 W respectively, while varying the pulsed current duty cycle from 17-50%. The author concluded that the electrode geometry contributed 45% to the surface finish while ultrasonic and pulsed current contributed 36% and 19% respectively.

Ultrasonic tool vibration was also investigated [7-9]. The authors reported a slight improvement in surface quality by ultrasonic vibrations of brass electrode when ECM of NC6 steel. The power of ultrasonic vibrations was varied between 20-120 W with maximum amplitude of 10 µm. The surface finish R_a was reduced from of 1.5 µm to 1.0 µm. When vibrating the electrode within 2-11 µm amplitude range, it was concluded that there exists specific amplitude to give optimum surface finish in different machining conditions. Later, these authors applied pulsed current and ultrasonic vibrations in their study. The power of ultrasonic vibrations was between 0-120 W and pulsed duration was between 1-9 ms. The best surface finish of ~ 0.2 µm R_a was achieved at 120 W power of ultrasonic vibrations and 1 ms pulsed duration (1 kHz).

The effect of ultrasonic vibrations was also studied experimentally and through computer simulation [10-11]. Noting that a resulted current was affected by specific inter-electrode gap, the study concluded that *MRR* was not effective when having ultrasonic vibration with large inter-electrode gap. The same authors later performed simulations of ultrasonically-assisted ECM using Computational Fluid Dynamics. In order to understand the influence of cavitation on the dissolution process, the author solved the problem of electrolyte flow when tool vibrated at 20 kHz frequency and different amplitudes up to 10 µm. It concluded that the pressure of electrolyte in the vicinity of anodic surface fluctuated between 50,000-200,000 bars when applying tool vibration at 5 µm and 50 µs period of vibration (20 kHz).

Ultrasonic vibration of microtool was also investigated [12]. A disk-shaped microtool was used for deep hole drilling experiments and for flushing enhancement. The improvement in hole quality was characterized by observing the change of overcut. At the machining feed rate of 100 µm/min, the radial overcut was reduced from 130 µm to ~50 µm when vibration was applied in the axial direction.

Electrochemical Jet Machining of titanium was investigated in another study [13]. Vibration of workpiece at 40 kHz was done with a transducer that received signals from a function generator. The change in surface oxide formation produced different surface finish; a 31 % reduction in surface roughness R_a was obtained due to ultrasonic vibration. There was a significant reduction of oxide layer formation when applying ultrasonic vibration to the titanium workpiece: 22% area of sample showed passive layer formation with use of ultrasonic vibration, compared to 45% area without vibration.

- Ultrasonic wave in electrolyte

Some researchers applied ultrasonic waves in the electrolyte instead of vibrating electrodes or workpiece. In reference [14] the authors studied the effect of conducting ECM in ultrasonic field by setting up an electrochemical cell in ultrasonic baths at either 20 kHz or 56 kHz. The effect of ultrasound wave was expected by the transmission of high frequency wave through the glass walls of the electrochemical cell. At a current of 10 A, the mass removal

rate increased from 0.194 g/min to 0.197 g/min when ECM at 20 kHz, the removal rate was further increased to 0.207 g/min at 56 kHz. However, insignificant results were obtained when experimented at 15 A. The study concluded that the small improvement was due to ineffective transmission of ultrasonic wave through glass wall into the inter-electrode gap of ECM cell; the cavitation through ultrasonic baths might not affect the ECM process as it does with normal cleaning of samples.

Most research works have been using ultrasonic vibration of tool or workpiece to obtain significant results. Although feasible in laboratory environment, such approach might not be practical or cost prohibitive in industrial applications. Mounting of ultrasonic actuators onto a large and heavy workpiece or intricate electrode might be expensive and technically difficult. If vibration of tool or workpiece is not precisely controlled, multiple mode shapes in high frequency vibration may result in dimensional inaccuracy of the fabricated workpiece. This research did not vibrate workpiece or electrode, but sending ultrasonic wave to a workpiece surface via flowing electrolyte.

3. Experiments

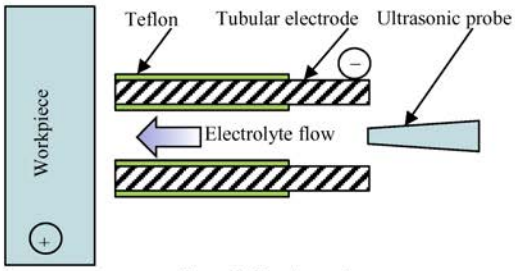

Figure 1. Experimental setup

Figure 1 illustrates the experimental setup where the cathodic electrode moves horizontally into an anodic workpiece. Electrolyte flowed around a sonicator probe, into the hollow electrode, and impacted perpendicularly onto the workpiece surface. A Branson SLPe ultrasonic probe (ϕ3.2 mm tip, 102 mm long) generated 40 kHz wave with adjustable amplitude from 0-70μm. A Longer WT2600-2J peristaltic pump was used to pump the electrolyte at 1.8 L/min, and a 2-axis Velmex BiSlide positioning system was used to control the position and speed of an electrode. The whole ECM cell was positioned on a rigid granite table for vibration isolation.

All experiments were conducted using aluminum 6061-T6 as workpiece (60 mm long x 50mm wide x 6.3 mm thick). Its chemical composition was 97.9 wt% Al, 0.3 Cr, 0.2 Cu, 1.0 Mg, and 0.6 Si. Holes were drilled with commercially Teflon coated stainless steel tubes (Ø9.5mm OD, 0.3mm wall thickness). The coating thickness was 0.1mm, and the length of the coated surface was 13 mm on both the outside and inside diameters of an electrode.

Potassium bromide (KBr, 1mol/L) was used as electrolyte. Each experimental run was started with electrolyte temperature in the range of 21-26 °C. Temperature of the electrolyte was measured before each experiment using a Raytek ST infrared pyrometer. Electrolyte conductivity, measured before each run using the Hannah HI 8733 conductivity meter, was in the range of 111-121 mS/cm. Although the metallic by-products in used electrolyte could be filtered using centrifugal method in small quantity, the settling method was used for a large quantity of used electrolyte. In the latter method the used electrolyte, mixed with metal debris and by-products, was stored in a separate container overnight so that the heavy metallic and salt by-products would be settled at the container bottom. The clear electrolyte at the top was separated and used for subsequent experiment if its conductivity was still comparable with that of the fresh electrolyte.

A full factorial experiment was conducted based on four input parameters for investigation of ultrasonic amplitude and other process parameters. Two replicates were made for each condition. The machining time was calculated based on tool feed rate of 10 or 15 µm/s to reach the same travel distance of 6.2 mm below the workpiece surface.

Table 1: Input parameter levels (* denotes a reference level)

Variable	Symbol	Level
Ultrasonic vibration amplitude (µm)	A_v	0*, 15, 36
Peak current (A)	I_p	22, 26
Pulsed current frequency (Hz)	f_c	0*, 125, 275
Machining time (min)	t_m	6.89, 10.33

After ECM'ed, all samples were rinsed and cleaned with water in an ultrasonic bath for 1 minute and then dried with compressed air. All samples were positioned in a glass beaker in the bath with ECM'ed holes facing downward to facilitate removal of residual particles from the holes.

The Alicona Infinite Focus 3D profiler was used to analyze ECM'ed hole profile. Typical 3D model was generated and was used to measure removed volume, surface roughness, and wall taper angle (Figure 2). Figure 3 shows the actual sectioned view of two holes that were ECM'ed at the same operating conditions, illustrating the repeatability of the experimental system.

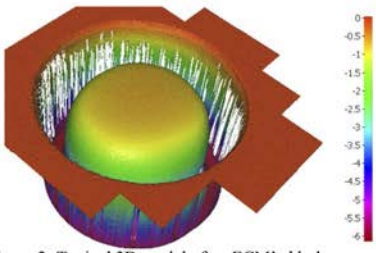

Figure 2: Typical 3D model of an ECM'ed hole (259.13 mm^3 removed volume).
Parameters: 0 A_v, 26A I_p, 275Hz f_c , 6.89min t_m

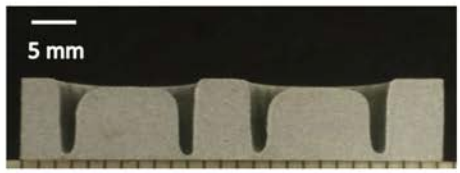

Figure 3: Cross sectional view of a pair of holes machined under same operating conditions.
Parameters: 36µm A_v, 22A I_p, 275Hz f_c, 6.89min t_m

a

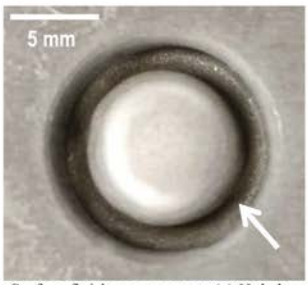

b

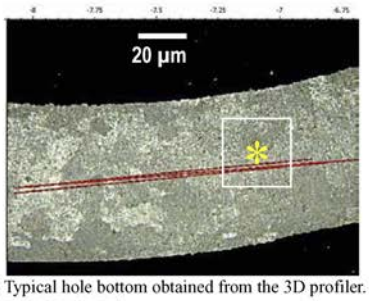

Figure 4: Surface finish measurement (a) Hole bottom at arrow, (b) Typical hole bottom obtained from the 3D profiler. The "*" shows group of 4-mm zigzag lines for line average roughness measurement.

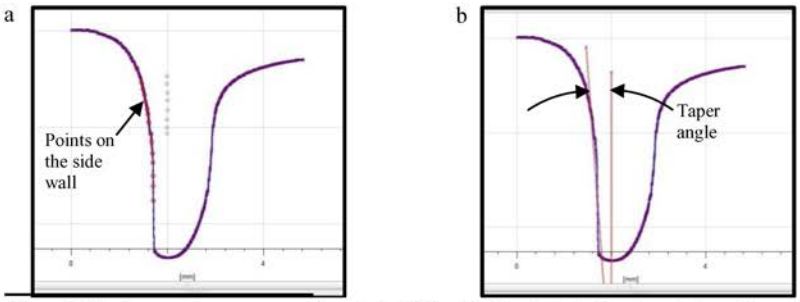

Figure 5: Hole taper angle measurement from typical 3D profile (a) point selection along hole profile and (b) best fit lines for taper angle measurement.

The flat bottom profile of an ECM'ed hole (Figure 4a) was captured with the Alicona (Figure 4b). A zigzag sectioning line (total 4-mm long) was drawn near the center of the groove and its line roughness was calculated. This procedure is repeated 5 times for each sample and 2 replicates to give a total of 10 measurements for R_a and R_z with each experimental condition. The top most location of an ECM'ed hole was measured for taper angle after obtaining the scanned profile (Figures 5a and b). After selecting 20 points on the side wall and another 20 points along a vertical line, the system then calculated the taper angle of the side wall.

To verify the accuracy of volume measurement, volume comparison was performed against the calculated volumes of simple holes. Three holes were drilled on a ground steel plate (40 mm x 60 mm x 3.30 mm thick) using a ø7.937 mm (ø5/16 inch) drill on a vertical milling machine. The holes were carefully deburred, and their volumes were measured on the Alicona to verify the accuracy. Five points were selected on each hole circumference for diameter calculation. The Minitab software was used to analyze data *MRR*, surface finish, and taper angle.

4. Results and Discussion

The following sections compare the volume measurement against calculated data, process efficiency in terms of hole profile and *MRR*, and hole quality in terms of surface finish and hole taper angle.

Although the Alicona is calibrated using a linear standard scale, we compared the measured volume against the calculated volumes to verify the system accuracy when scanning and calculating volume of a three-dimensional object. Volume of a cylindrical hole after drilling on a ground plate was calculated from its geometry. The volume is simply:

$$V = \frac{\pi d^2}{4} t \tag{2}$$

Where:

V: hole volume (mm^3)
d: hole diameter (mm)
t: plate thickness (mm)

Table 2 shows the result of volume calculation and measurement in the comparison study. The measured hole diameters (ϕ8.46 mm average) were slightly larger than the drill diameter (ϕ7.937 mm) due to slight out of round of the drill bit and runout spindle of the milling machine. Despite of this, the difference between averaged volume measuring from three drilled holes and that from profiler's measurement is merely 0.5%.

Table 2: Volume comparative results

Hole #	Hole depth (mm)	Average hole diameter (mm)	Calculated hole volume (mm^3)	Measured hole volume (mm^3)	Error (%)
1	3.30	8.44	184.53	185.55	+0.55
2	3.30	8.48	186.26	185.06	-0.64
3	3.30	8.46	185.55	185.49	-0.03

Since the workpiece is polycrystalline 6061 aluminum, it is assumed that the major alloying element aluminum (97.9 wt %) is ionized and reacts with the electrolyte to form by-products while ignoring insignificant by-products from other alloying elements. The overall reaction of aluminum in KBr solution is:

$$2Al + 6H_2O + KBr \rightarrow 2Al^{3+} + 3H_2 + 6OH^- + K^+ + Br^- \quad (3)$$

The aluminum ions then combine with bromide ions to form either dialuminum hexabromide Al_2Br_6, or the more stable aluminum tribromide $AlBr_3$ as by-products.

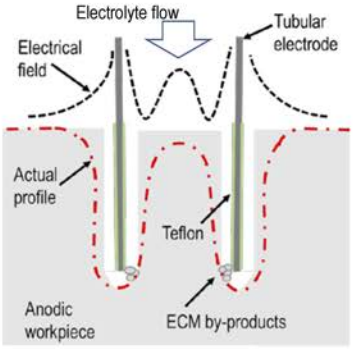

Figure 6: Electrical field and actual profile of an ECM'ed hole.

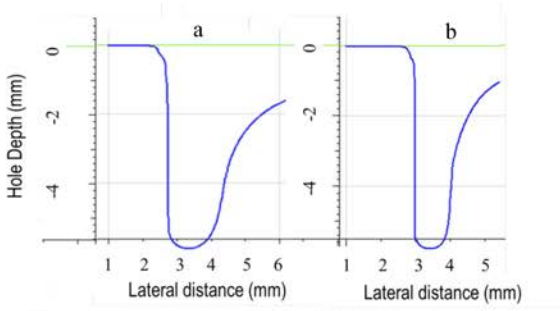

Figure 7: Side wall profile of a hole after (a) 10.33 min and (b) 6.89 min to reach 6.2 mm hole depth.
Parameters: 0 A_v, 22 A I_p, 125 Hz f_c

The electrical field strength between a circular electrode and a flat plate can be derived [15] and schematically shown in Figure 6. The highest field strength is along a circular ring directly below the tubular electrode; the field strength is diminishing outward and away from the tube wall, but is additive to form a pronounced peak at the tubular electrode center. The result is a strong current directly below the electrode, an average current in the central region, and a weaker stray current at positions away from the electrode.

Teflon was chosen as insulating material for ECM since this material is stable to withstand the thermal and chemical conditions during ECM. Although insulation would be effectively to reduce stray current, a thick electrode insulator tends to delaminate during ECM and interferes with deep drilling process. On the other hand, a very thin insulator is costly, quickly eroded by fast flowing by-products. An optimal insulating Teflon layer of 0.1 mm was chosen in this study.

The resulted hole profile now can be explained. Significant material is removed directly below the electrode, while the corners and center position of a hole are rounded off due to weaker stray current (Figures 3-5). The agglomerated by-product particles –assuming $AlBr_3$–, are present in a small gap between electrode and workpiece, and interfere with the ion transport mechanism if they are not effectively flushed away. However, the flushed particles in fast flow electrolyte would erode and enlarge the overcut of the ECM'ed profile, and round off the sharp entrance corners. Qualitative results and effects of process parameters are discussed in the following sections.

4.1. Material removal rate

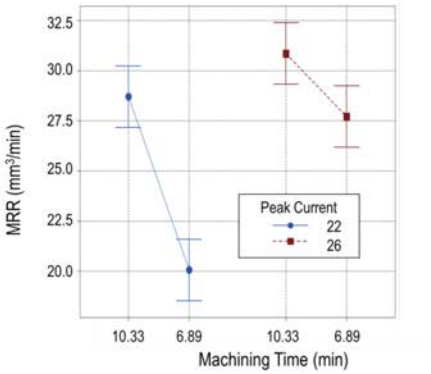

Figure 8: Effect of peak current and machining time on MRR.
Parameters: 125 Hz f_c, 36 µm A_v

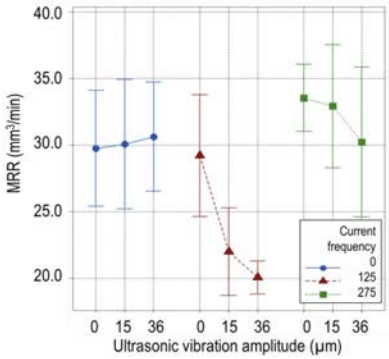

Figure 9: Effect of pulsed frequency and ultrasonic wave amplitude on MRR.
Parameters: 22 A I_p, 15 µm/s f_r

An electrode was programmed to move at different feed rates of 10 or 15 µm/s to reach the same travel distance of 6.2 mm, the machining times were 10.33 and 6.89 minutes respectively. A longer machining time allows stray current to remove more materials in lateral directions and material in the center of the tubular electrode (Figure 7). Figures 8 and 9 show the effects of MRR by machining times, peak current, pulsed current frequencies, and ultrasonic amplitudes. A longer machining time and higher current result in higher MRR as expected and shown in Figure 8. The Faraday's law in equation (1) states that the material removal is proportional to the electrical charge; therefore, a uniform direct current (DC) would theoretically provide a higher MRR. However, the MRR from pulsed current at 22 A, 275 Hz is consistently higher than that at 22 A DC (Figure 9). This is due to better flushing of the by-products during off-time and perhaps the lower temperature between electrodes when pulsed current is used instead of a constant DC current.

An attempt to further enhancing MRR when coupling pulsed current and ultrasonic wave, however, was not successful. The MRR was slightly enhanced when both DC current and ultrasonic wave were applied, yet decreased when both pulsed current and ultrasonic wave were used (Figure 9). When applying an ultrasonic wave in electrolyte of an ECM system, the following cavitation actions are hypothesized [16-17]:

- Bubbles are nucleated in electrolyte that grow, but eventually collapse and generating shockwave at approximately 5,000°K and pressure in the range of 2,000 atm in the electrolyte, and
- Bubbles are nucleated at tool and workpiece surfaces that grow and implode to form micro-jets that impact the solid surface at velocity reaching 280 m/s.

Although the above simulated results (magnitudes of pressure, temperature, and velocity) would depend on the specific electrolyte and ultrasonic parameters, it is assumed that similar phenomena would happen in other ECM systems. High velocity microjet directing perpendicular onto the anodic workpiece surface and intense shockwave pressure would impede ionization process, therefore reduce ionizing rate of the workpiece and decrease the MRR.

Similar conclusions on the effect of ultrasonic vibration on MRR were also cited by other researchers. The MRR was not significantly affected by ultrasonic vibration of tool in ECM [3, 10] or sending ultrasonic wave in electrolyte bath [14]. Although having different material removal mechanisms, both ECM and electrical discharge machining (EDM) have common challenge in effective removal of debris between narrow inter-electrode gaps. A

study concluded that the MRR in EDM reduced when applying ultrasonic vibration at 16 µm amplitude and 100 Hz frequency [18].

Based on the experimental data, a regression model for main effects of input parameters on MRR is proposed. The R^2 value of this linear model is 66.78%.

$$MRR = 9.71 - 0.2317\,A_v + 0.699\,I_p + 0.02277\,f_c + 0.292\,t_m \quad (4)$$

Where

MRR	: Material removal rate (mm^3/min)
A_v	: Ultrasonic wave amplitude (µm)
I_p	: Peak pulsed current (A)
f_c	: Pulsed current frequency (Hz)
t_m	: Machining time (min)

Equation (4) predicts that the peak pulsed current is the most important contributing factor to MRR, following by the machining time. The ultrasonic amplitude has negative effect on MRR.

4.2. Hole quality

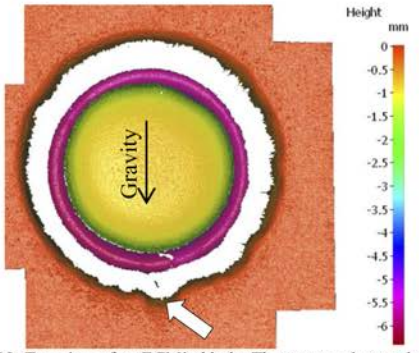

Figure 10: Top view of an ECM'ed hole. The arrow points to the eroded area located at the lowest position.
Parameters: 26A I_p, 36µm A_v, 125Hz f_c, and 6.89 min t_m

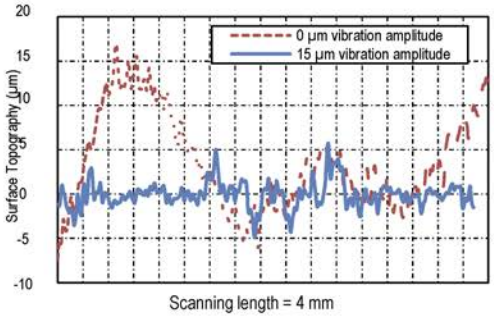

Figure 11: Typical roughness profile along the 4-mm scanning length.
Parameters: 275Hz f_c, 22A I_p, and 6.89 min t_m

During a long machining time, more material inside the tubular electrode is removed due to higher electrical field strength and additive stray current. The insoluble $AlBr_3$ particles would follow the fast flowing electrolyte at a fast speed of 0.5 m/s (1.8 L/min though a ϕ8.7 mm tubular electrode) from center of the electrode down to bottom of the hole then moving upward to outside of the hole. The hole quality is affected not only by the conditions for ion removal from the anodic workpiece, but also the inevitable erosion of the by-product particles in fast moving electrolyte. Since the hole and electrode axes are horizontal and concentric, the lowest position of a hole would experience the highest flow density of the relatively heavy $AlBr_3$ by-product (3.2 g/cm^3 density). Evidence of erosion is seen at the lowest position of an ECM'ed hole (Figure 10). Hole quality assessment, therefore, is measured at the highest location of a hole. Typical surface asperities at hole bottom are shown in Figure 11.

Both hole profile and surface finish are considered for hole quality investigation. Erosion is the main factor contributing to hole taper when using insulated electrodes as in this study. The highest taper angles of ~11° were resulted when ECM'ing with DC current without ultrasonic wave (Figure 12). By applying pulsed currents at 125 or 275 Hz, then the hole taper angles were significantly reduced to be ~3°. The cyclic on/off time period of pulsed current allowed the smaller by-product particles to form and move along the side wall of a hole, therefore reducing

erosion damage and taper angle. Breaking up the by-product particles by ultrasonically-induced cavitation further reduced the erosion of particle and improved the taper angle. Sharp taper angles of ~1° were repeatedly measured when ECM'ing at high pulsed frequency of 40 kHz ultrasonic wave with amplitude of 15-36 µm.

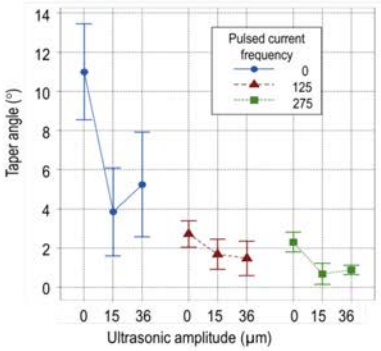

Figure 12: Effect of pulsed frequency and ultrasonic amplitude on hole taper angle.
Parameters: 22A I_p, 6.89 min t_m

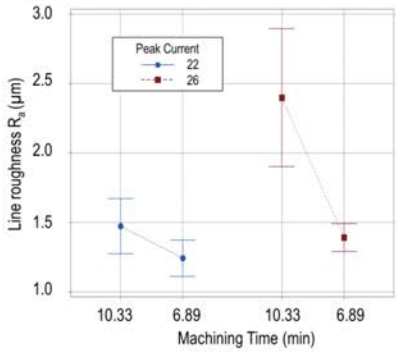

Figure 13: Effect of peak current and machining time on roughness.
Parameters: 275Hz f_c, and 36µm A_v

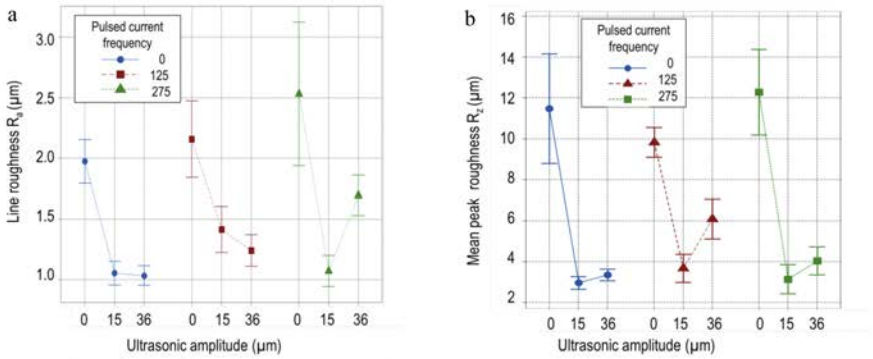

Figure 14: Effect of pulsed frequency and ultrasonic amplitude on (a) line roughness R_a and (b) mean peak roughness R_z.
Parameters: 22 A I_p and 6.89 min t_m

The very fine particles of $AlBr_3$ –induced by combination of pulsed current and ultrasonic wave at hole central area– flowed thought inter-electrode gap (bottom of a hole) before flowing out of a hole. Such fine particles would polish the hole bottom surface as evidenced from Figure 11. A higher current removed more material (higher MRR as shown in Figure 8). Since the polycrystalline workpiece possesses grains in random directions, it is expected that surface finish would be higher due to different removal rates from one grain to its neighboring grains and at the grain boundaries. When generating ultrasonic wave at higher amplitude of 36 µm, the surface cavitation imploded and formed microjets directing into the workpiece surface and damaging the workpiece surface; the result was poorer surface finish during long ECM'ing time and higher peak current (Figure 13). Assuming insignificant microjet effect when applying ultrasonic wave at 15 µm amplitude, the polishing effect of fine $AlBr_3$ particles would improve the surface finish. Both surface finish measurements of R_a and R_z reduced significantly to almost one order of magnitude. However, the cavitation-induced microjet dominated at higher ultrasonic amplitude of 36 µm and degraded the surface finish (Figures 14a and b). The results agreed with published literature that part quality improves when using ultrasonic in ECM. The reference [12] reported an improvement of microhole quality when measuring surface finish, hole taper, and radial overcut. The reference [19] concluded that the impact of microjets

due to ultrasonic cavitation would have significant effects on the chemical composition and physical morphology; therefore, affect surface quality and dissolution rate.

Data from surface finish measurement were analyzed. By excluding the data at high ultrasonic amplitude 36µm, a regression model, with R^2 value of 94.41%, is shown below.

$$R_a = 1.707 - 0.11579\,A_v + 0.0148\,I_p + 0.1053\,t_m - 0.000482\,f_c \quad (5)$$

Where

R_a : Average line surface roughness (µm)
A_v : Ultrasonic wave amplitude (µm)
I_p : Pulsed peak current (A)
f_c : Pulsed current frequency (Hz)
t_m : Machining time (min)

Equation (5) predicts a smoother surface (smaller R_a value) is contributed by the ultrasonic amplitude below 36µm, and pulsed current frequency below 275 Hz. A high peak current and long machining time would degrade the surface finish.

5. Conclusions and recommendations

This research study combines pulsed current and ultrasonic vibration in electrochemical machining of 6061 aluminum alloy. It has been shown that:

1) Embedding ultrasonic wave in fast flowing electrolyte is more practical than ultrasonically vibrating a large workpiece or electrode.
2) Electrochemical machining can be enhanced by combining pulsed current and ultrasonic wave. The combination improves hole quality at the expense of material removal rate.
3) De-agglomeration of $AlBr_3$ by-products at optimal pulsed current and ultrasonic wave reduces the average surface roughness from ~2.5 µm to 1 µm, and the wall taper angle from ~11° to ~1°.
4) Cavitation-induced microjets interfere with ionization process. At high ultrasonic power, the high impacting velocity of microjets on the anodic surface reduces material removal rate, worsens surface finish, and might damage it with micro-pitting.

Although a full factorial experiment was performed in this study, a more comprehensive experiment with 5-level central composite design would be more accurate to predict the effect of pulsed current and ultrasonic wave. Future work would include simulation study on how ultrasonic parameters affecting microjets and the resulted pitting corrosion on ECM surface.

References

[1] K. P. Rajurkar, J. Kozak, B. Wei, J. A. McGeough, Study of pulse electrochemical machining characteristics. CIRP Annals - Manufacturing Technology, 42(1) (1993) 231-234.
[2] B. Bhattacharyya, J. Munda, M. Malapati, Advancement in electrochemical micro-machining. Journal of Machine Tools and Manufacture, 44(15) (2004) 1577-1589.
[3] B. Bhattacharyya, M. Malapati, J. Munda, A. Sarkar, Influence of tool vibration on machining performance in electrochemical micro-machining of copper. Journal of Machine Tools and Manufacture, 47(2) (2007) 335-342.
[4] P. S. Pa, Design of effective plate-shape electrode in ultrasonic electrochemical finishing. Journal of Advanced Manufacturing Technology, 34(1-2) (2006) 70-78.
[5] P. S. Pa, Electrode form design of large holes of die material in ultrasonic electrochemical finishing. Journal of Materials Processing Technology (2007) 470-477.
[6] P. S. Pa, Super finishing with ultrasonic and magnetic assistance in electrochemical micro-machining. Electrochimica Acta, 54(25) (2009) 6022-6027.

[7] A. Ruszaj, M. Zybura-Skrabalak, S. Skoczypiec, R. Żurek. Electrochemical machining supported by electrode ultrasonic vibrations. In Proceedings of the 13th International Symposium for Electromachining, (2001).
[8] A. Ruszaj, M. Zybura, R. Zurek, G. Skrabalak. Some aspects of the electrochemical machining process supported by electrode ultrasonic vibrations optimization. Journal of Engineering Manufacture, 217(10) (2003) 1365-1371.
[9] A. Ruszaj, S. Skoczypiec, J. Czekaj, T. Miller, J. Dziedzic, Surface micro and nanofinishing using pulse electrochemical machining process assisted by electrode ultrasonic vibrations. In Proceedings of the 15th International Symposium on Electromachining–ISEM XV (2007).
[10] S. Skoczypiec, A. Ruszaj, Discussion of cavitation phenomena influence on electrochemical machining process. Journal of Manufacturing Science and Technology, 7(2) (2005) 27-32.
[11] S. Skoczypiec, Research on ultrasonically assisted electrochemical machining process. Journal of Advanced Manufacturing Technology, 52(5-8) (2010) 565-574.
[12] M. Wang, Y. Zhang, Z. He, W. Peng, Deep micro-hole fabrication in EMM on stainless steel using disk micro-tool assisted by ultrasonic vibration. Journal of Materials Processing Technology, 229 (2016) 475-483.
[13] J. Mitchell-Smith, A.T. Clare, Electrochemical jet machining of titanium: Overcoming passivation layers with ultrasonic assistance. Procedia CIRP, 42 (2016) 379-383.
[14] D. Nicoară, A. Hedeş, I. Şora, Ultrasonic enhancement of an electrochemical machining process. In Proceedings of the 5th WSEAS international conference on Applications of Electrical Engineering (2006).
[15] R. A. Serway, J. W. Jewett, Physics for Scientists and Engineers with Modern Physics: Nelson Education, (2013).
[16] Hielscher, Ultrasonic production of nano-size dispersions and emulsions. arXiv preprint arXiv:0708.1831, (2007).
[17] Hielscher, https://www.hielscher.com/ultrasonic-cavitation-in-liquids-2.htm. Access 10 November 2016.
[18] E. Uhlmann, D. C. Domingos, Investigations on vibration-assisted EDM-machining of seal slots in high-temperature resistant materials for turbine components. Procedia CIRP, 6 (2013) 71-76.
[19] S. Sebastian, R. Adam, C. Jan, Z. S. Maria, Primary investigations on USECM–CNC process (2003).